

Constraining the spin and the deformation parameters from the black hole shadow

Naoki Tsukamoto, Zilong Li and Cosimo Bambi¹

Center for Field Theory and Particle Physics & Department of Physics,
Fudan University, 220 Handan Road, 200433 Shanghai, China

E-mail: tsukamoto@fudan.edu.cn, zilongli@fudan.edu.cn, bambi@fudan.edu.cn

Abstract. Within 5-10 years, very-long baseline interferometry (VLBI) facilities will be able to directly image the accretion flow around SgrA*, the super-massive black hole candidate at the center of the Galaxy, and observe the black hole “shadow”. In 4-dimensional general relativity, the no-hair theorem asserts that uncharged black holes are described by the Kerr solution and are completely specified by their mass M and by their spin parameter a . In this paper, we explore the possibility of distinguishing Kerr and Bardeen black holes from their shadow. In Hioki & Maeda (2009), under the assumption that the background geometry is described by the Kerr solution, the authors proposed an algorithm to estimate the value of a/M by measuring the distortion parameter δ , an observable quantity that characterizes the shape of the shadow. Here, we try to extend their approach. Since the Hioki-Maeda distortion parameter is degenerate with respect to the spin and possible deviations from the Kerr solution, one has to measure another quantity to test the Kerr black hole hypothesis. We study a few possibilities. We find that it is extremely difficult to distinguish Kerr and Bardeen black holes from the sole observation of the shadow, and out of reach for the near future. The combination of the measurement of the shadow with possible accurate radio observations of a pulsar in a compact orbit around SgrA* could be a more promising strategy to verify the Kerr black hole paradigm.

Keywords: gravity, modified gravity, astrophysical black holes.

¹Corresponding author

Contents

1	Introduction	1
2	Black hole shadow	3
3	Measuring the Kerr spin parameter from the observation of the shadow	6
4	Measuring the spin and the deformation parameters from the observation of the shadow	9
4.1	Distortion parameter ϵ	9
4.2	Position of the center of the shadow	10
4.3	Radius of the shadow R	10
5	Discussion	10
6	Summary and conclusions	14

1 Introduction

In 4-dimensional general relativity, the no-hair theorem guarantees that uncharged black holes (BHs) are only described by the Kerr solution, which is completely specified by two parameters; that is, the BH mass M and the BH spin angular momentum J [1–3]. A fundamental limit for a Kerr BH is the bound $|a| \leq M$, where $a = J/M$ is the BH spin parameter¹. This is just the condition for the existence of the event horizon. Astrophysical BH candidates are stellar-mass compact objects in X-ray binary systems and super-massive bodies at the center of every normal galaxy [4]. They are thought to be the Kerr BHs of general relativity simply because they cannot be explained otherwise without introducing new physics, but there is no evidence that the spacetime around them is described by the Kerr metric.

In the last decade, there have been both significant theoretical work to understand the accretion process onto BH candidates and new observational facilities, so that it might be possible to test the actual nature of these objects in a near future from the properties of the electromagnetic radiation emitted by the accreting material [5, 6]. A large number of methods have been proposed, including the study of the thermal spectrum of thin accretion disks [7–10], the analysis of the $K\alpha$ iron line [11–13], the observation of the so-called quasi-periodic oscillations (QPOs) [14–17], the measurement of the radiative efficiency [18–21], and the estimate of the jet power [22–24]. The main difficulty to achieve this goal is that the properties of the electromagnetic radiation from a Kerr BH with dimensionless spin parameter a/M can be very similar, and practically indistinguishable, from the ones of non-Kerr objects with different spin. In other words, it is usually impossible to constrain at the same time the value of the spin parameter and possible deviations from the Kerr solution. For some metrics, the combination of the analysis of the disk’s thermal spectrum and of the $K\alpha$ iron line cannot break the degeneracy between the spin and the deformation parameters, while in other cases that can be achieved only with very good measurements [25]. The combination

¹Throughout the paper, we use units in which $G_N = c = 1$, unless stated otherwise.

of the analysis of the thermal spectrum of thin disks and the estimate of the jet power can potentially do the job [23, 24], but the latter is not yet a mature technique and therefore it cannot yet be used to test fundamental physics. The result is that right now we can only rule out the possibility that BH candidates are some kinds of very exotic objects, like some types of wormholes [26] or some exotic compact objects without event horizon [27, 28]. The non-observation of electromagnetic radiation emitted by the possible surface of these objects may also be interpreted as an indication for the existence of an event horizon [29, 30] (but see [31, 32]). However, more reasonable alternatives, like non-Kerr BHs, are difficult to test.

Recent observations of SgrA* at mm wavelength suggest that, hopefully within about 5 years, very-long baseline interferometry (VLBI) facilities at mm/sub-mm wavelength will be able to directly image the accretion flow around the super-massive BH candidate at the center of our Galaxy with a resolution of the order its gravitational radius $r_g = M$ [33, 34]. These observations will open a completely new window to test gravity in the strong field regime and, in particular, to verify if SgrA* is a Kerr BH, as expected from general relativity. The main goal of these experiments is the observation of the “shadow” of SgrA*. The shadow of a BH is a dark area over a brighter background observed by directly imaging the accretion flow around the compact object [35, 36]. While the intensity map of the image depends on complicated astrophysical processes related to the accretion properties and the emission mechanisms, the exact shape of the shadow is only determined by the background geometry, being the apparent photon capture sphere as seen by a distant observer. A very accurate detection of the boundary of the shadow can thus provide information on the geometry around SgrA* and test the Kerr BH hypothesis. Starting from Refs. [37, 38], a number of tests has been proposed in the literature and shadows in different background metrics have been calculated by different groups [39–46]. For a recent review, see e.g. Ref. [47].

At first approximation, the shape of the shadow is a circle. The radius of the circle corresponds to the apparent photon capture radius, which, for a given metric, is set by the mass of the compact object and its distance from us. For SgrA* and for the other nearby super-massive BH candidates, these two quantities are currently not known with good precision, and therefore the observation of the size of the shadow may not be used to test the spacetime geometry around the compact object (but see Ref. [45] and the conclusions of the present work). The shape of the shadow is usually thought to be the key-point. The first order correction to the circle is due to the spin, as the photon capture radius is different for co-rotating and counter-rotating particles. The boundary of the shadow has thus a dent on one side: the deformation is more pronounced for an observer on the equatorial plane (viewing angle $i = 90^\circ$) and decreases as the observer moves towards the spin axis, to completely disappear when $i = 0^\circ$ or 180° . Possible deviations from the Kerr solutions usually introduce smaller corrections and therefore they can be detected only in the case of excellent data.

In Ref. [48], two of us have studied the measurement of the Kerr spin parameter of Kerr BHs and non-Kerr regular BHs; that is, we measured the spin parameter a/M from the shape of the shadow of a BH assuming it was a Kerr BH. We used the procedure proposed in Ref. [49], which is based on the determination of the distortion parameter $\delta = D/R$, where D and R are, respectively, the dent and the radius of the shadow. In the case of non-Kerr BHs, this technique provides the correct value of a/M for non-rotating objects, but a quite different spin for near extremal states. If we compare this measurement with the frequency of the innermost stable circular orbit (ISCO) that can be potentially obtained by the observations of blobs of plasma orbiting around the BH candidate [50], we find that the nature of the object may be tested in the case of a non-rotating or slow-rotating BHs,

while that seems to be impossible for near extremal states, as the two techniques essentially provide the same information on the spacetime geometry.

In the present paper, we consider a different approach to test the Kerr geometry around SgrA*. We assume to have good observational data of the BH shadow and we try to measure two parameters. One parameter of the shadow can indeed only determine one parameter of the background geometry, which is enough in the case of the Kerr metric where there is only the spin. If we want to test the Kerr nature of the BH candidate, the spacetime metric will be also characterized by one (or more) deformation parameter(s), measuring possible deviations from the Kerr solution. In general, the Hioki-Maeda distortion parameter δ is degenerate with respect to the spin and the deformation parameters, in the sense that the same value of δ is found for any deformation parameter for a particular value of a/M . With the measurement of another parameter of the shadow, it is possible to break such a degeneracy and eventually test the Kerr metric of the spacetime. We explore three possibilities. We introduce a second distortion parameter, ϵ , which characterizes possible deviations from the shape of the shadow of a Kerr BH. While a similar approach may sound the most natural extension of Ref. [49], it turns out that Kerr BHs and non-Kerr regular BHs have very similar shapes and such a small difference is very difficult to detect in true observational data. We thus consider the possibility of measuring the off-set of the center of the shadow with respect to the actual position of the BH. Even in this case, the approach can potentially distinguish Kerr BHs and non-Kerr regular BHs, but an accurate measurement of the BH position is very challenging, at least now. The third and last case is the measurement of the radius of the shadow, R . Here, we need good measurements of the BH mass and distance from us, which are definitively not available today, but they could be possible in the future, for instance from accurate radio observations of a pulsar orbiting SgrA* with a period shorter than 1 year. The same pulsar could also provide a precise estimate of the spin parameter (obtained in the weak field), to be compared with the Hioki-Maeda distortion parameter δ of the strong gravity regime. It seems therefore that the sole observation of the shadow cannot distinguish Kerr and Bardeen BHs, while the combination of the shadow and pulsar observations is more promising to probe the geometry around SgrA*.

The content of the paper is as follows. In Section 2, we review the calculation of the BH shadow, while in Section 3 we review the procedure proposed in Ref. [49] to infer the spin parameter from the determination of the distortion parameter δ . In Section 4, we explore the possibility of testing the Kerr metric from the combination of the estimates of the Hioki-Maeda distortion parameter δ with, respectively, the distortion parameter ϵ , the position of the center of the shadow with respect to the one of the BH, and the shadow radius R . Section 5 is devoted to the discussion. Summary and conclusions are in Section 6.

2 Black hole shadow

If a BH is surrounded by an optically thin and geometrically thick accretion flow, a distant observer sees a dark area over a brighter background. Such a dark area is the “shadow” of the BH. The boundary of the shadow corresponds to the apparent image of the photon capture sphere and therefore it only depends on the geometry of the background [35, 36]. In this section, we briefly review the calculation of the BH shadow. In the case of the Kerr

metric, the line element in Boyer-Lindquist coordinates is

$$ds^2 = - \left(1 - \frac{2Mr}{\Sigma} \right) dt^2 - \frac{4aMr \sin^2 \theta}{\Sigma} dt d\phi + \frac{\Sigma}{\Delta} dr^2 + \Sigma d\theta^2 + \left(r^2 + a^2 + \frac{2a^2 Mr \sin^2 \theta}{\Sigma} \right) \sin^2 \theta d\phi^2, \quad (2.1)$$

where

$$\Sigma = r^2 + a^2 \cos^2 \theta, \quad \Delta = r^2 - 2Mr + a^2, \quad (2.2)$$

M is the BH mass, and $a = J/M$. The photon motion is governed by the equations [35]

$$\Sigma \left(\frac{dt}{d\lambda} \right) = \frac{AE - 2aMrL_z}{\Delta}, \quad (2.3)$$

$$\Sigma^2 \left(\frac{dr}{d\lambda} \right)^2 = \mathcal{R}, \quad (2.4)$$

$$\Sigma^2 \left(\frac{d\theta}{d\lambda} \right)^2 = \Theta, \quad (2.5)$$

$$\Sigma \left(\frac{d\phi}{d\lambda} \right) = \frac{2aMrE + (\Sigma - 2Mr) L_z \csc^2 \theta}{\Delta}, \quad (2.6)$$

where λ is an affine parameter, and

$$\mathcal{R} = E^2 r^4 + (a^2 E^2 - L_z^2 - \mathcal{Q}) r^2 + 2M [(aE - L_z)^2 + \mathcal{Q}] r - a^2 \mathcal{Q}, \quad (2.7)$$

$$\Theta = \mathcal{Q} (a^2 E^2 - L_z^2 \csc^2 \theta) \cos^2 \theta, \quad (2.8)$$

$$A = (r^2 + a^2)^2 - a^2 \Delta \sin^2 \theta. \quad (2.9)$$

E and L_z are, respectively, the conserved photon energy and the conserved component of the photon angular momentum parallel to the BH spin. \mathcal{Q} is the Carter constant

$$\mathcal{Q} = p_\theta^2 + \cos^2 \theta \left(\frac{L_z^2}{\sin^2 \theta} - a^2 E^2 \right), \quad (2.10)$$

and $p_\theta = \Sigma \frac{d\theta}{d\lambda}$ is the canonical momentum conjugate to θ .

Motion is only possible when $\mathcal{R}(r) \geq 0$, and therefore the analysis of the position of the roots of $\mathcal{R}(r)$ can be used to distinguish the capture from the scattered orbits. The three kinds of photon orbits are:

1. *Capture orbits*: $\mathcal{R}(r)$ has no roots for $r \geq r_+$, where r_+ is the radial coordinate of the BH event horizon. In this case, photons come from infinity and then cross the horizon.
2. *Scattering orbits*: $\mathcal{R}(r)$ has real roots for $r \geq r_+$, which correspond to the photon turning points. If the photons come from infinity, they reach a minimum distance from the BH, and then go back to infinity.
3. *Unstable orbits of constant radius*: these orbits separate the capture and the scattering orbits and are determined by

$$\mathcal{R}(r_*) = \frac{\partial \mathcal{R}}{\partial r}(r_*) = 0, \quad \text{and} \quad \frac{\partial^2 \mathcal{R}}{\partial r^2}(r_*) \geq 0, \quad (2.11)$$

where r_* is the larger real root of \mathcal{R} .

The boundary of the shadow of a BH can be determined by finding the unstable orbits of constant radius.

Since the photon trajectories are independent of the photon wavelength, it is convenient to introduce the parameters $\xi = L_z/E$ and $\eta = Q/E^2$. ξ and η are related to the “celestial coordinates” α and β of the image plane of the distant observer by

$$\alpha = \frac{\xi}{\sin i}, \quad \beta = \pm(\eta + a^2 \cos^2 i - \xi^2 \cot^2 i)^{1/2}, \quad (2.12)$$

where i is the angular coordinate of the observer at infinity. Every photon orbit can be characterized by the constants of motion ξ and η . The boundary of the BH shadow is represented by a closed curve determined by the set of unstable circular orbits (ξ_c, η_c) on the plane of the distant observer. From Eqs. (2.7) and (2.11), the equations determining the unstable orbits of constant radius are

$$\begin{aligned} \mathcal{R} &= r^4 + (a^2 - \xi_c^2 - \eta_c)r^2 + 2M[\eta_c + (\xi_c - a)^2]r - a^2\eta_c = 0, \\ \frac{\partial \mathcal{R}}{\partial r} &= 4r^3 + 2(a^2 - \xi_c^2 - \eta_c)r + 2M[\eta_c + (\xi_c - a)^2] = 0. \end{aligned} \quad (2.13)$$

In the Schwarzschild background ($a = 0$), the BH shadow is a circle of radius

$$R = 3\sqrt{3}M \approx 5.196M. \quad (2.14)$$

If $a \neq 0$, one finds

$$\begin{aligned} \xi_c &= \frac{M(r_*^2 - a^2) - r_*(r_*^2 - 2Mr_* + a^2)}{a(r_* - M)}, \\ \eta_c &= \frac{r_*^3[4a^2M - r_*(r_* - 3M)^2]}{a^2(r_* - M)^2}, \end{aligned} \quad (2.15)$$

where r_* is the radius of the unstable orbit. The shadow of Kerr BHs can be found in many papers in the literature [49].

In the present work, we want to figure out how we can distinguish Kerr and Bardeen BHs from the observation of the BH shadow. In Boyer-Lindquist coordinates, the line element of the rotating Bardeen metric has the same form as the Kerr one, Eqs. (2.1) and (2.2), with the mass M replaced by m [51, 52]:

$$M \rightarrow m = M \left(\frac{r^2}{r^2 + g^2} \right)^{3/2}, \quad (2.16)$$

without changing a (at least in the simplest form, see Ref. [52] for more details). Here g can be interpreted as the magnetic charge of a non-linear electromagnetic field² or just as a quantity introducing a deviation from the Kerr solution. The position of the even horizon is still given by the largest root of $\Delta = 0$ and there is a bound on the maximum value of the spin parameter, above which there are no BHs. The maximum value of a/M is 1 for $g/M = 0$ (Kerr case), and decreases as g/M increases, to reach 0 for $g/M = \sqrt{16/27} \approx 0.7698$. There are no BHs for $g/M > \sqrt{16/27}$. The situation is similar to the Kerr-Newman solution, where the maximum value of a/M is 1 for a vanishing electric charge Q (Kerr case), and decreases

²As found in Ref. [51], the Bardeen metric can be obtained as an exact solution of Einstein’s equations coupled to a non-linear electromagnetic field. The latter allows to avoid the no-hair theorem.

as Q increases, to reach 0 for $Q/M = 1$. The Bardeen metric can be seen as the prototype of a large class of metrics, in which the line element in Boyer-Lindquist coordinates has the same form as the Kerr one, with M replaced by a function $m(r)$ that depends only on the radial coordinate. Such a family of metrics includes the Kerr-Newman solution, in which $m = M - Q^2/2r$.

Since the Bardeen metric (as well as all the other metrics in this family) has the same nice properties as the Kerr one, in particular there exists the Carter constant \mathcal{Q} and the equations of motion are separable in Boyer-Lindquist coordinates, it is straightforward to generalize the above calculations of the shadow of a Kerr BH to the Bardeen case. The system in Eq. (2.13) is replaced by

$$\begin{aligned}\mathcal{R} &= r^4 + (a^2 - \xi_c^2 - \eta_c)r^2 + 2m[\eta_c + (\xi_c - a)^2]r - a^2\eta_c = 0, \\ \frac{\partial \mathcal{R}}{\partial r} &= 4r^3 + 2(a^2 - \xi_c^2 - \eta_c)r + 2m[\eta_c + (\xi_c - a)^2] = 0,\end{aligned}\tag{2.17}$$

with m given by Eq. (2.16) and f defined by

$$f = 1 + \frac{r}{m} \frac{dm}{dr} = \frac{r^2 + 4g^2}{r^2 + g^2}.\tag{2.18}$$

The counterpart of Eq. (2.15) is

$$\begin{aligned}\xi_c &= \frac{m[(2-f)r_*^2 - fa^2] - r_*(r_*^2 - 2mr_* + a^2)}{a(r_* - fm)}, \\ \eta_c &= \frac{r_*^3\{4(2-f)a^2m - r_*[r_* - (4-f)m]^2\}}{a^2(r_* - fm)^2},\end{aligned}\tag{2.19}$$

with $m = m(r_*)$ and $f = f(r_*)$. Example of shadows of Bardeen BHs are reported in Ref. [48]. Let us note that Eq. (2.19) does not hold only for the Bardeen metric, but in the large class of BH solutions in which the line element is given by Eqs. (2.1) and (2.2) with M replaced by some $m(r)$ that depend on the radial coordinate only.

3 Measuring the Kerr spin parameter from the observation of the shadow

The boundary of the BH shadow corresponds to the apparent image of the photon capture sphere as seen by the distant observer and it is only determined by the background geometry. If we want to infer the value of the parameters of the metric, it is convenient to figure out the features of the shadow that better characterize its shape and that can be measured from the shadow image. This strategy was first proposed in [49] to estimate the value of the spin parameter a/M from the observation of the shadow of a Kerr BH. In this section, we will briefly review their approach, while in the next section it will be extended to test the Kerr metric of BH candidates.

At first approximation, the boundary of the shadow is a circle, and it is exactly a circle in the case of a static spherically symmetric solution (like the Schwarzschild metric) or in the one of a stationary axisymmetric solution in which the distant observer is located along the symmetry axis (like the Kerr metric and a viewing angle $i = 0^\circ$ or 180°). We can thus approximate the shadow with a circle passing through the three points located, respectively,

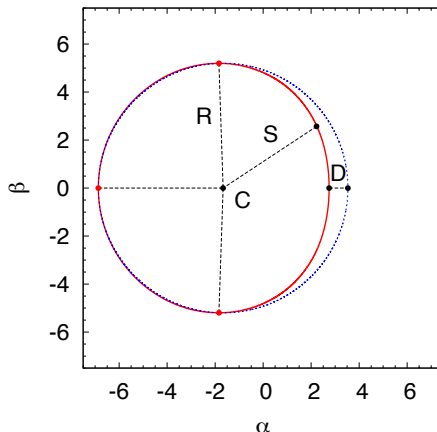


Figure 1. BH shadow with the three parameters that approximately characterize its shape: the radius R , the dent D , and the distance S . R is defined as the radius of the circle passing through the three red points, located at the top ($\beta = \beta_{\max}$), bottom, and most left end of the shadow. D is the difference between the most right points of the circle and of the shadow. S is the distance between the center of the circle, C , and the most right end of the shadow at $\beta = \beta_{\max}/2$. The Hioki-Maeda distortion parameter is $\delta = D/R$. The second distortion parameter is $\epsilon = S/R$. α and β in units $M = 1$. See the text for more details.

at the top position, bottom position, and most left end of its boundary (the three red points in Fig. 1). The radius of the shadow, R , is defined as the radius of this circle.

The first order correction to the circle is due to the spin, because of the spin-orbit coupling between the photon and the BH. The gravitational force is indeed stronger if the photon angular momentum is antiparallel to the BH spin (the photon capture radius is thus larger), and weaker in the opposite case (the photon capture radius is smaller). The result is that the shadow has a dent on one side, which is larger for a viewing angle $i = 90^\circ$, and reduces as the distant observer move to the axis of symmetry, to completely disappear when $i = 0^\circ$ or 180° . We define the dent D as the distance between the right endpoints of the circle and of the shadow, see Fig. 1. We can then introduce the Hioki-Maeda distortion parameter $\delta = D/R$, which is a quantity that can be measured from the image of the shadow and can be used to characterize its shape [49].

If we know that the spacetime geometry is described by the Kerr solution and we have an independent estimate of the viewing angle i , the measurement of the distortion parameter provides an estimate of the BH spin parameter a/M . Indeed, for a give i , there is a one-to-one correspondence between a/M and δ , and the function $\delta(a/M)$ can be inverted to obtain $a/M|_{\text{Kerr}}(\delta)$. If we relax the Kerr BH hypothesis and we want to test the nature of the BH candidate, we have to introduce at least one parameter that quantifies possible deviations from the Kerr geometry. If we adopt the Bardeen metric, this role is played by the Bardeen charge g . Now the boundary of the shadow, as well as all the other properties of the background metric at small radii, depends on both a/M and g/M . The distortion parameter is $\delta(a/M, g/M)$ and it is not possible to infer a/M without an independent estimate of g/M . If we assume that the object is a Kerr BH even if $g/M \neq 0$, we can determine the so-called Kerr spin parameter

$$a/M|_{\text{Kerr}} = a/M|_{\text{Kerr}}[\delta(a/M, g/M)], \quad (3.1)$$

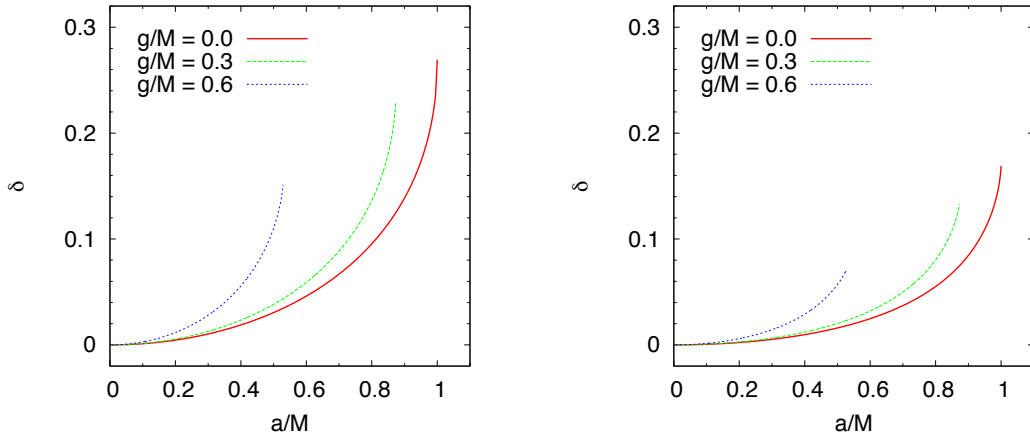


Figure 2. Hioki-Maeda distortion parameter δ as a function of the spin parameter a/M for Kerr BHs (red solid line), Bardeen BHs with $g/M = 0.3$ (green dashed line), and Bardeen BHs with $g/M = 0.6$ (blue dotted line). The inclination angle is $i = 90^\circ$ (left panel) and 45° (right panel). The maximum value of the Hioki-Maeda distortion parameter is $\delta = 7/26 \approx 0.269$ in the case of an extremal Kerr BH ($a/M = 1$) and a viewing angle $i = 90^\circ$.

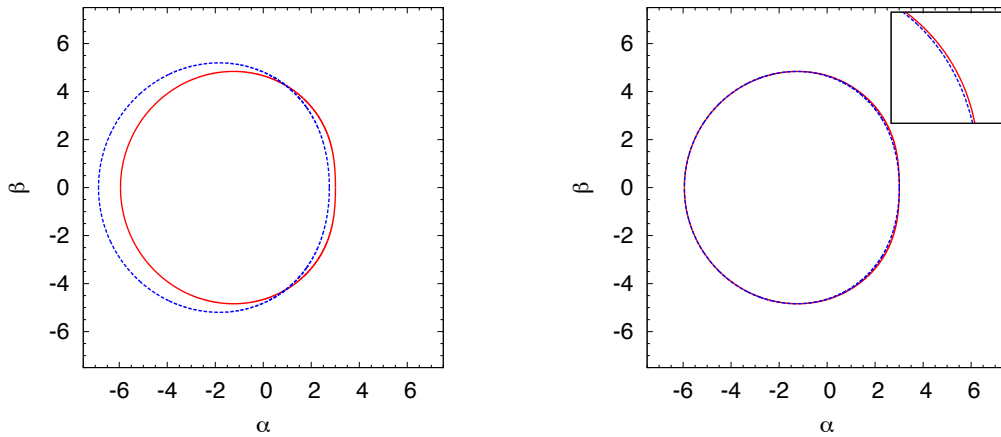


Figure 3. Left panel: shadows of a Kerr BH (blue dashed line) and of a Bardeen BH with $g/M = 0.6$ (red solid line) with the same mass $M = 1$, the same viewing angle $i = 90^\circ$, and the same Hioki-Maeda distortion parameter $\delta = 0.1500$. The Kerr BH has $a/M = 0.9189$, while the Bardeen BH has $a/M = 0.5286$. Right panel: as in the left panel, but for two BHs with the same shadow radius R on the sky ($M = 0.9311$ for the Kerr BH, $M = 1$ for the Bardeen one) and the same position of the center of the circle C (the shadow of the Kerr BH has been shifted by 0.433 along the α direction). See the text for more details.

which provides a wrong value of the spin for $a/M \neq 0$ [48]. Fig. 2 shows the Hioki-Maeda distortion parameter δ as a function of the BH spin parameter a/M for the case of Kerr BHs and Bardeen BHs with $g/M = 0.3$ and 0.6 . It is clear that the same distortion parameter δ can characterize the shadow of a Kerr BH with spin a/M or of a Bardeen BH with lower spin.

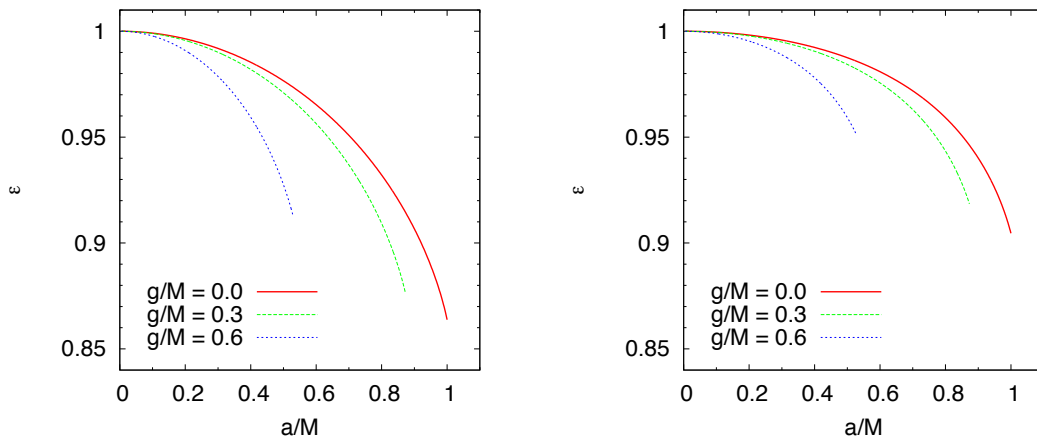


Figure 4. Distortion parameter ϵ as a function of the spin parameter a/M for Kerr BHs (red solid line), Bardeen BHs with $g/M = 0.3$ (green dashed line), and Bardeen BHs with $g/M = 0.6$ (blue dotted line). The inclination angle is $i = 90^\circ$ (left panel) and 45° (right panel).

4 Measuring the spin and the deformation parameters from the observation of the shadow

Since the Hioki-Maeda distortion parameter δ is degenerate with respect to the BH spin and possible deviations from the Kerr solution (and it could not be otherwise, because one parameter of the shadow can at most be used to determine one parameter of the background geometry), in this section we look for the best choice of the second parameter to test the Kerr metric. If we consider non-rotating BHs, the shadow is a circle for any value of g/M and the sole difference is its radius, which depends on g/M . For $a/M \neq 0$, we can expect that shadows with the same Hioki-Maeda distortion parameter have different shape and that the difference increases as g/M and a/M increase and i approaches 90° . As first step, it is useful to visualize such a difference. This is done in Fig. 3, where we compare the shadows of a Kerr BH and of a Bardeen BH with $g/M = 0.6$ for $i = 90^\circ$. We start from imposing that $\delta = 0.1500$. We find that such a distortion parameter corresponds to a Kerr BH with $a/M = 0.9189$ and to a $g/M = 0.6$ Bardeen BH with $a/M = 0.5286$. The left panel shows the two shadows as computed using the same BH mass M . The right panel compares the two shadows after properly rescaling the one of the Kerr BH and shifting it on the celestial plane, so that their radii have the same value and the centers of the shadows coincide. We note that the maximum value of the spin for a Bardeen BH with $g/M = 0.6$ is $a/M \approx 0.5295$, so we are considering an almost extremal BH.

4.1 Distortion parameter ϵ

From the right panel in Fig. 3, we can realize that the main difference in the shadow shape is in the apparent photon capture radii on the right side, corresponding to the ones associated to corotating orbits. We are thus tempted to define the distortion parameter ϵ as follows. With reference to Fig. 1, we call S the distance between the center of the circle of the shadow, C , and the point on the right side of the boundary with coordinate $\beta = \beta_{\max}/2$, where β_{\max} is the β coordinate of the top end of the shadow used to find R . We then define $\epsilon = S/R$ which, like the Hioki-Maeda distortion parameter δ , only depends on the shape of the shadow. The

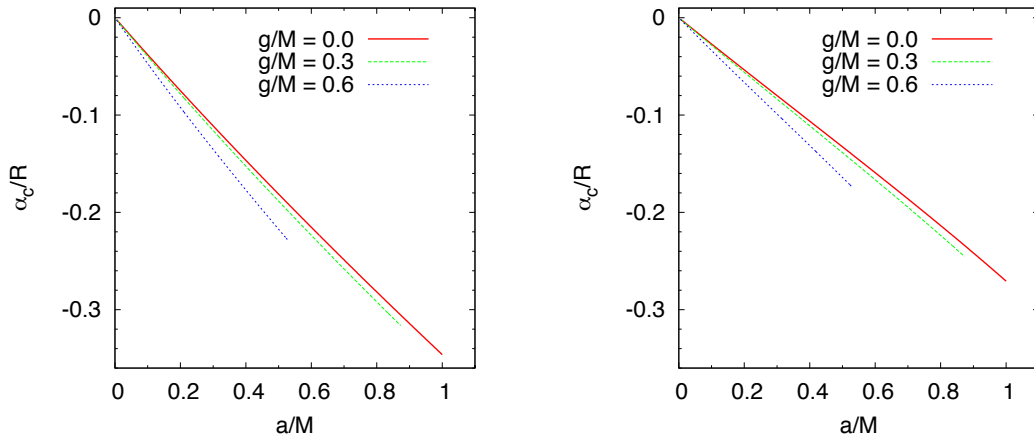


Figure 5. Position of the center of the circle on the sky as a function of the spin parameter a/M for Kerr BHs (red solid line), Bardeen BHs with $g/M = 0.3$ (green dashed line), and Bardeen BHs with $g/M = 0.6$ (blue dotted line). The inclination angle is $i = 90^\circ$ (left panel) and 45° (right panel).

distortion parameter ϵ as a function of the spin parameter a/M for Kerr BHs, Bardeen BHs with $g/M = 0.3$, and Bardeen BHs with $g/M = 0.6$ is shown in Fig. 4.

4.2 Position of the center of the shadow

The shapes of the shadows of Kerr and Bardeen BHs are clearly very similar and therefore only very accurate image can distinguish the two metrics and provide a meaningful constraint on g/M . One can therefore try to follow a different strategy from the exact determination of the shadow shape. The left panel in Fig. 3 may suggest that this could be achieved from the estimate of the exact position on the sky of the center of the circle, C , with respect to the actual center of the system, $\alpha = \beta = 0$. In principle, that is surely an available option and Fig. 5 shows α_c/R as a function of the spin parameter for the shadows of Kerr and Bardeen BHs. We have plotted α_c/R instead of α_c or α_c/M because in this way we do not assume an accurate measurement of the BH mass and distance. We just need a very good measurement of the BH position on the sky.

4.3 Radius of the shadow R

Lastly, we consider the possibility that we can get very good estimates of the BH mass and distance and we can therefore combine the Hioki-Maeda distortion parameter δ with the measurement of the radius of the shadow R . R/M as a function of the spin parameter a/M for $g/M = 0.0$ (Kerr), 0.3, and 0.6 is shown in Fig. 6. It is remarkable that for an observer near the equatorial plane the value of R/M is mainly determined by g/M and it is not very sensitive to the spin. The dependence of R on the spin increases as the observer moves towards the axis of symmetry, but it is still weak for $i = 45^\circ$, as shown the right panel in Fig. 6.

5 Discussion

At least in principle, the simultaneous measurement of the Hioki-Maeda distortion parameter δ and one of the three parameters discussed in the previous section (ϵ , α_c , or R) breaks the

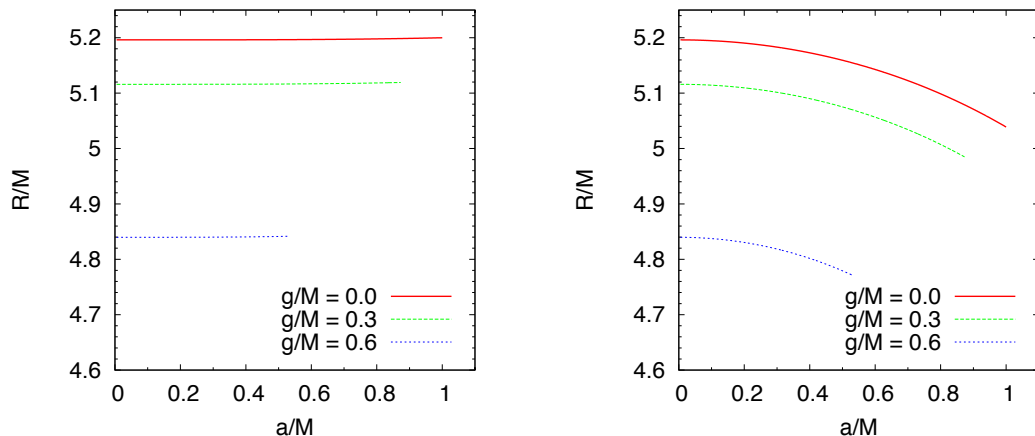


Figure 6. Radius of the shadow R/M as a function of the spin parameter a/M for Kerr BHs (red solid line), Bardeen BHs with $g/M = 0.3$ (green dashed line), and Bardeen BHs with $a/M = 0.6$ (blue dotted line). The inclination angle is $i = 90^\circ$ (left panel) and 45° (right panel).

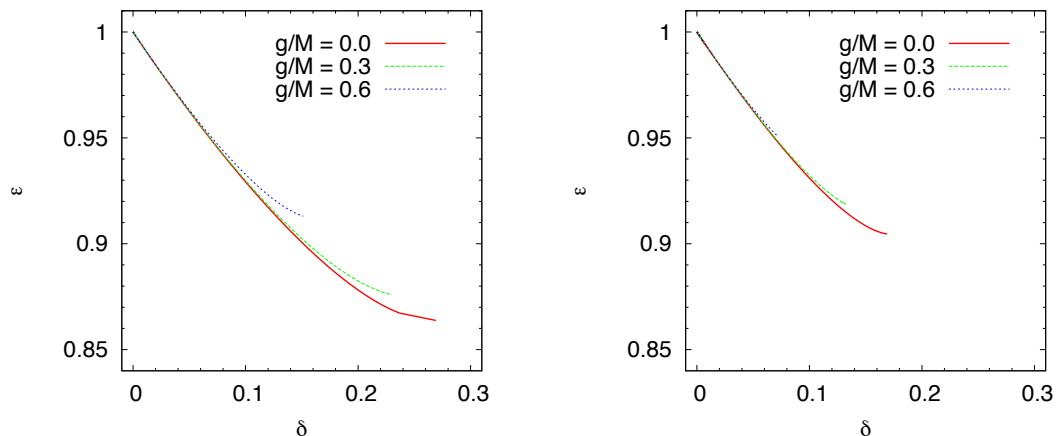


Figure 7. The Hioki-Maeda distortion parameter δ against the distortion parameter ϵ for Kerr BHs (red solid line), Bardeen BHs with $g/M = 0.3$ (green dashed line), and Bardeen BHs with $a/M = 0.6$ (blue dotted line). The inclination angle is $i = 90^\circ$ (left panel) and 45° (right panel).

degeneracy between the BH spin and possible deviations from the Kerr geometry and it is therefore a potential approach to test the Kerr metric around SgrA* from the observation of its shadow. This is more evident if we plot the Hioki-Maeda distortion parameter against one of the other three. The plots are shown in Fig. 7 for the distortion parameter ϵ , in Fig. 8 for the shadow center α_c/M , and in Fig. 9 for the shadow radius R/M . The fact that these curves depend on the value of g/M is enough to conclude that there is no degeneracy. However, the above consideration is correct only in principle, in the sense that we have also to check if it is possible to measure ϵ , α_c , or R with sufficient precision to distinguish Kerr and Bardeen BHs.

In the case of the distortion parameter ϵ , the difference between Kerr and Bardeen BHs is clearly tiny, as it was already evident from Fig. 3. Even in the most optimistic case of an inclination angle $i = 90^\circ$, for the same Hioki-Maeda distortion parameter δ the difference

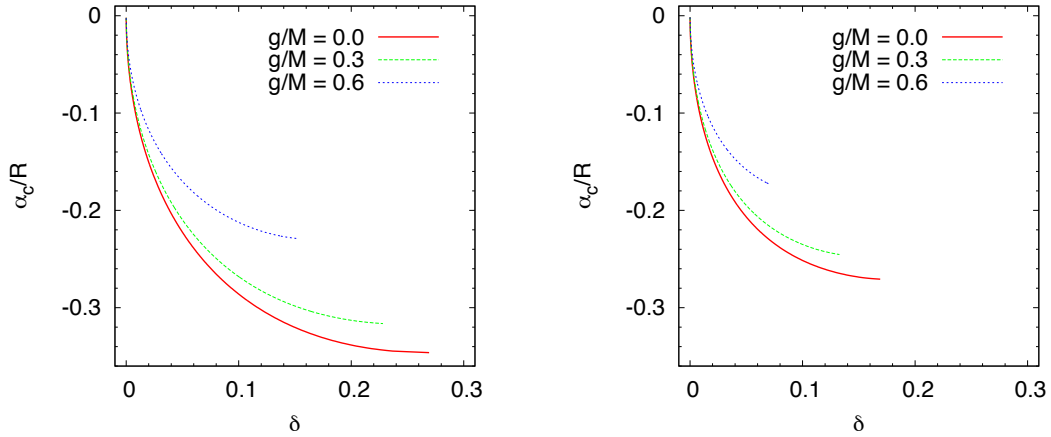


Figure 8. The Hioki-Maeda distortion parameter δ against the position of the center of the circle on the sky for Kerr BHs (red solid line), Bardeen BHs with $g/M = 0.3$ (green dashed line), and Bardeen BHs with $a/M = 0.6$ (blue dotted line). The inclination angle is $i = 90^\circ$ (left panel) and 45° (right panel).

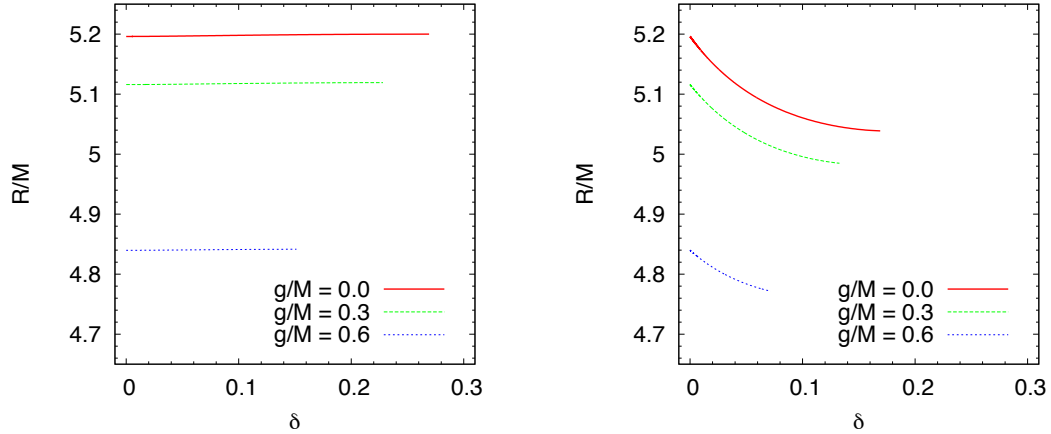


Figure 9. The Hioki-Maeda distortion parameter δ against the radius of the shadow R/M for Kerr BHs (red solid line), Bardeen BHs with $g/M = 0.3$ (green dashed line), and Bardeen BHs with $a/M = 0.6$ (blue dotted line). The inclination angle is $i = 90^\circ$ (left panel) and 45° (right panel).

between the parameter ϵ for Kerr BHs and Bardeen BHs with $g/M = 0.3$ is never larger than 0.8%, lower 0.2% for $\delta < 0.15$, and lower than 0.08% for $\delta < 0.10$. If we compare Kerr BHs and Bardeen BHs with $g/M = 0.6$, we find that shadows with the same δ have ϵ parameters that differ less than 1.5% (but it is close to 1.5% only when the Bardeen BH is an almost extremal object). Such precisions are at least extremely challenging, even in the most favorable conditions for a/M , g/M , and i . The uncertainties on δ and ϵ are

$$\frac{\Delta\delta}{\delta} = \frac{\Delta R}{R} + \frac{\Delta D}{D}, \quad \frac{\Delta\epsilon}{\epsilon} = \frac{\Delta R}{R} + \frac{\Delta S}{S}, \quad (5.1)$$

where ΔR , ΔD , and ΔS are the uncertainties on R , D , and S . For SgrA*, we expect $R \approx 30 \mu\text{as}$. With an imaging resolution of $\sim 0.3 \mu\text{as}$, $\Delta\epsilon/\epsilon$ is already 2% or worst, which is not enough even to distinguish a Kerr from a Bardeen BH with $g/M = 0.6$. Here we are

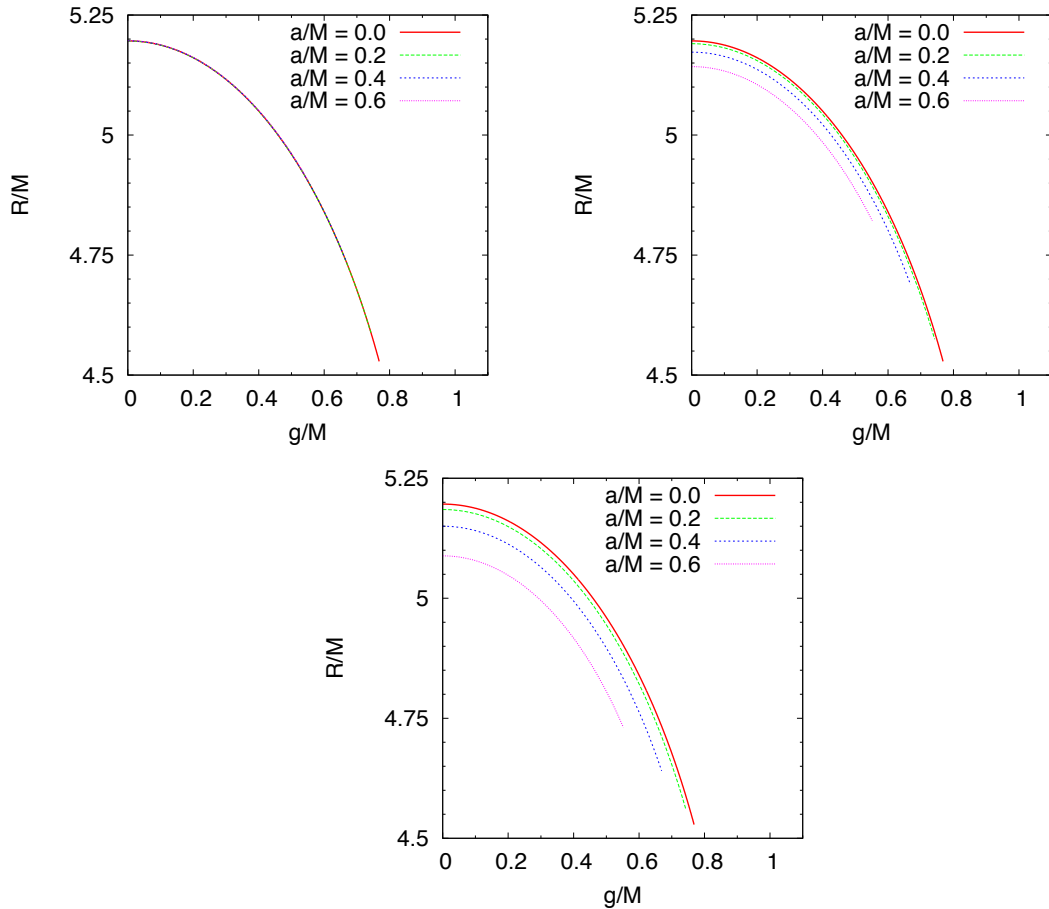


Figure 10. The radius of the shadow R/M as a function of the Bardeen charge g/M for different values of the spin parameter and an observer inclination angle $i = 90^\circ$ (top left panel), 45° (top right panel), and 10° (bottom panel).

also assuming to know the inclination angle i with arbitrary precision, which is surely not the case and its uncertainty introduces an additional error in the estimate of ϵ . The fact that the shapes of the shadows in Kerr and non-Kerr spacetimes are usually very similar, and therefore difficult to distinguish with observations, was already stressed in Ref. [39] from the comparison of Kerr and Tomimatsu-Sato shadows. Other non-Kerr metrics might have shadows with more significant deviations, but more often the difference seems to be very small.

The measurement of the shift between the position of the center of the shadow and the actual center of the system may initially look more promising, because Fig. 8 shows that the lines for different values of g/M have a large separation. Unfortunately, the position of the center of the system on the sky is very difficult to determine and the uncertainty is $\Delta\alpha_c \sim 1$ mas (but see Ref. [53], where a position relative to a reference point with an accuracy of order $1 \mu\text{as}$ might be possible).

The last parameter of the shadow discussed in the previous section is the apparent size of the radius R (see Figures 9 and 10). In this case, we need very good measurement of the BH mass and distance from us. At present, these quantities are difficult to measure and the

final uncertainty on the expected apparent size on the sky of R is around 15% [45]. Such an uncertainty is larger than the difference between the radius of the shadow of a Kerr BH and of a Bardeen BH with $g/M = 0.6$ with the same δ , which is around 7% for $i = 90^\circ$ and independently of the spin parameter a/M .

The measurement of the radius of the shadow may turn out to be the most promising approach in the case of significant improvements of the estimate of the BH mass and of our distance from the galactic center. That could be achieved in the case of the discovery of a radio pulsar in a compact orbit (i.e. with an orbital period of a few months) around SgrA*. As discussed in Ref. [54], pulsar timing can determine the Keplerian and Post-Keplerian parameters and therefore get a robust estimate of the BH mass, independently of the distance from us from the galactic center, which can instead be inferred with high precision by combining the BH mass with near-infrared astrometric measurements. In this case, the uncertainty on R would be determined by the imaging resolution. If the resolution is at the level of $0.3 \mu\text{as}$, R can be measured with a precision of 1%. If SgrA* is rotating rapidly, after a few years of observations of the radio pulsar, the spin parameter a/M could be determined with a precision of order 0.1% (but the uncertainty would be significantly larger for a mid-rotating or slow-rotating BH) [54]. Such a measurement could also be combined with the ones of δ and R on the spin-Bardeen charge plane. Since the pulsar is relatively far from the BH, the pulsar measurement of the frame dragging is really sensitive to the value of a/M , independently of the nature of the SgrA*, because possible deviations from the Kerr solution are suppressed by powers in $M/r \ll 1$, where r is the distance of the pulsar³.

The possible constraints from the simultaneous measurements of the Hioki-Maeda distortion parameter δ , the shadow radius R/M , and the spin parameter a/M from a radio pulsar in the case of a Kerr BH with $a/M = 0.7$ are shown in Fig. 11. The left panel is for an observer’s viewing angle $i = 90^\circ$, while the right panel for $i = 45^\circ$. For a Kerr BH with $a/M = 0.7$, the Hioki-Maeda distortion parameter is $\delta = 0.0668$ ($i = 90^\circ$) and 0.0371 ($i = 45^\circ$). The red dashed-dotted line in Fig. 11 indicates the objects with the same Hioki-Maeda distortion parameter, and the two blue dashed lines on the two sides are the boundary of the allowed region assuming an uncertainty on δ of 20%⁴. In the same way, the shadow radius for a similar BH is $R/M = 5.20$ ($i = 90^\circ$) and $R/M = 5.12$ ($i = 45^\circ$), the red dashed-dotted line is the central value, while the two blue dashed lines are the boundary of the allowed region assuming an uncertainty on R/M of 1%. In the case of the spin parameter a/M inferred from a radio pulsar, the uncertainty is assumed to be 1%.

6 Summary and conclusions

Within the next decade, VLBI facilities at mm/sub-mm wavelength will be able to directly image the accretion flow around SgrA*, the super-massive BH candidate at the center of our Galaxy, and open a new window to test gravity in the strong field regime. In particular, it will be possible to observe the BH “shadow”, whose boundary corresponds to the apparent image of the photon capture sphere and it is therefore determined by the spacetime geometry around the compact object.

³While pulsar timing can also measure the BH quadrupole moment and thus test the Kerr nature of SgrA* (at least in the case of a fast-rotating BH) [54], the combination of the measurement of the shadow and of the pulsar can test if there are deviations of higher order.

⁴In the case $i = 90^\circ$, the plot shows just one blue dashed line for R/M because there are no BHs with R/M 1% larger than the one of Kerr BHs.

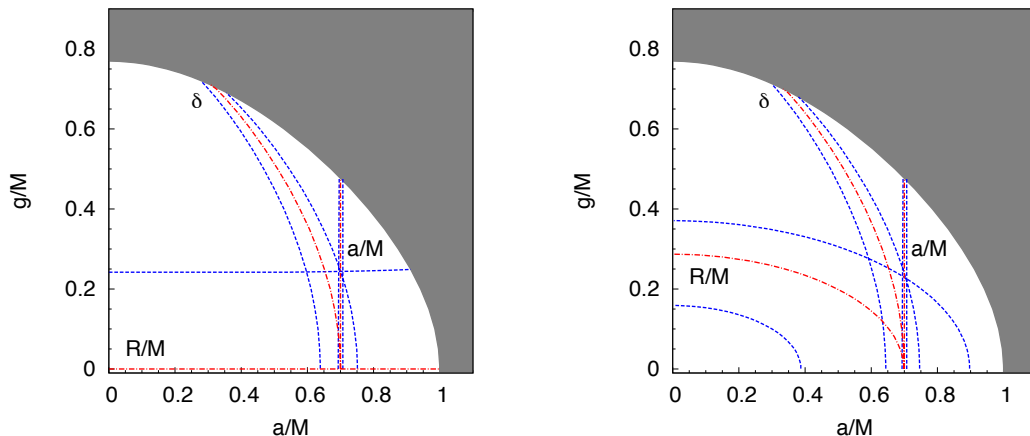


Figure 11. Hypothetical constraints from the measurements of the Hioki-Maeda distortion parameter δ determined with a precision of 20%, of the shadow radius R/M determined with a precision of 1%, and of the spin parameter a/M inferred from the orbital motion of a pulsar in a compact orbit and determined with a precision of 1%, assuming that the object is a Kerr BH with $a/M = 0.7$ and the inclination angle is $i = 90^\circ$ (left panel, in this case $\delta = 0.0668$ and $R/M = 5.20$) and 45° (right panel, in this case $\delta = 0.0371$ and $R/M = 5.12$). The red dashed-dotted lines are the central values of the measurements, while the blue dashed curves correspond to their uncertainties. The gray area is the region of objects without event horizon and can be ignored.

At first approximation, the shadow of a BH is a circle, and its radius depends on the BH mass, distance, and also on the background metric. The first order correction to the circle is due to the BH spin, because the photon capture radius is larger for photons with angular momentum antiparallel to the BH spin (the gravitational force is stronger), and smaller in the opposite case (the gravitational force is weaker). The final result is that the shadow shows a dent on one side. The magnitude of this dent can be measured in terms of the Hioki-Maeda distortion parameter δ [49]. The measurement of δ can be used to infer one parameter of the background geometry. If the compact object is a Kerr BH and we have an independent estimate of the inclination angle i , δ depends only on the BH spin parameter, and therefore its measurement can be used to infer a/M . If we want to test the Kerr BH hypothesis, we need to measure another parameter of the shadow in order to break the degeneracy between the spin and possible deviations from the Kerr solution.

In this work, we have focused the attention on the Bardeen metric, which is characterized by the Bardeen charge g and reduces to the Kerr solution for $g = 0$. The Bardeen solution can be seen as the prototype of a large class of non-Kerr BH metrics, in which the line element in Boyer-Lindquist coordinates is the same as the Kerr case with the mass M replaced by a function of the radial coordinate m , which reduces to M at large radii. We have investigated how it is possible to constrain the value of g/M from the observation of the BH shadow. We have explored three possibilities: the introduction of another distortion parameter of the shadow, ϵ , the determination of the center of the shadow with respect to the actual position of the BH, and the estimate of the shadow radius. While all the three approaches are at least challenging, the third one may be the most promising in the case of significant improvements of the measurement of the mass of SgrA* and of our distance from the galactic center. Since that can be achieved by discovering a radio pulsar with an orbital period of a few months around SgrA*, we have also briefly discussed the combination of the measurements of the

shadow and of the orbital motion of a similar pulsar. Such a synergy could turn out a quite interesting tool to test the nature of the super-massive BH candidate at the center of our Galaxy, because the shadow is sensitive to the strong gravitational field very close to the compact object, while the pulsar can accurately probe the weak field at relatively large distances.

While our calculations have been done in the specific case of the Bardeen background, we stress that it is straightforward to repeat our study for any BH spacetime in which there is the Carter constant and the photon equations of motion are separable. The main conclusion of this work are valid even for those BHs.

Acknowledgments

We thank Tomohiro Harada for useful comments and suggestions. This work was supported by the NSFC grant No. 11305038, the Shanghai Municipal Education Commission grant for Innovative Programs No. 14ZZ001, the Thousand Young Talents Program, and Fudan University.

References

- [1] B. Carter, *Phys. Rev. Lett.* **26**, 331 (1971).
- [2] D. C. Robinson, *Phys. Rev. Lett.* **34**, 905 (1975).
- [3] P. T. Chrusciel, J. L. Costa and M. Heusler, *Living Rev. Rel.* **15**, 7 (2012) [arXiv:1205.6112 [gr-qc]].
- [4] R. Narayan, *New J. Phys.* **7**, 199 (2005) [gr-qc/0506078].
- [5] C. Bambi, *Mod. Phys. Lett. A* **26**, 2453 (2011) [arXiv:1109.4256 [gr-qc]].
- [6] C. Bambi, *Astron. Rev.* **8**, 4 (2013) [arXiv:1301.0361 [gr-qc]].
- [7] D. F. Torres, *Nucl. Phys. B* **626**, 377 (2002) [hep-ph/0201154].
- [8] C. Bambi and E. Barausse, *Astrophys. J.* **731**, 121 (2011) [arXiv:1012.2007 [gr-qc]].
- [9] C. Bambi, *Astrophys. J.* **761**, 174 (2012) [arXiv:1210.5679 [gr-qc]].
- [10] C. Bambi, *Phys. Lett. B* **730**, 59 (2014) [arXiv:1401.4640 [gr-qc]].
- [11] Y. Lu and D. F. Torres, *Int. J. Mod. Phys. D* **12**, 63 (2003) [astro-ph/0205418].
- [12] T. Johannsen and D. Psaltis, *Astrophys. J.* **773**, 57 (2013) [arXiv:1202.6069 [astro-ph.HE]].
- [13] C. Bambi, *Phys. Rev. D* **87**, 023007 (2013) [arXiv:1211.2513 [gr-qc]].
- [14] T. Johannsen and D. Psaltis, *Astrophys. J.* **726**, 11 (2011) [arXiv:1010.1000 [astro-ph.HE]].
- [15] C. Bambi, *JCAP* **1209**, 014 (2012) [arXiv:1205.6348 [gr-qc]].
- [16] A. N. Aliev, G. D. Esmer and P. Talazan, *Class. Quant. Grav.* **30**, 045010 (2013) [arXiv:1205.2838 [gr-qc]].
- [17] C. Bambi, arXiv:1312.2228 [gr-qc].
- [18] C. Bambi, *Phys. Rev. D* **83**, 103003 (2011) [arXiv:1102.0616 [gr-qc]].
- [19] C. Bambi, *Phys. Lett. B* **705**, 5 (2011) [arXiv:1110.0687 [gr-qc]].
- [20] C. Bambi, *Phys. Rev. D* **85**, 043001 (2012) [arXiv:1112.4663 [gr-qc]].
- [21] Z. Li and C. Bambi, *JCAP* **1303**, 031 (2013) [arXiv:1212.5848 [gr-qc]].

- [22] R. Narayan and J. E. McClintock, *Mon. Not. Roy. Astron. Soc.* **419**, L69 (2012) [arXiv:1112.0569 [astro-ph.HE]].
- [23] C. Bambi, *Phys. Rev. D* **85**, 043002 (2012) [arXiv:1201.1638 [gr-qc]].
- [24] C. Bambi, *Phys. Rev. D* **86**, 123013 (2012) [arXiv:1204.6395 [gr-qc]].
- [25] C. Bambi, *JCAP* **1308**, 055 (2013) [arXiv:1305.5409 [gr-qc]].
- [26] C. Bambi, *Phys. Rev. D* **87**, 084039 (2013) [arXiv:1303.0624 [gr-qc]].
- [27] C. Bambi and D. Malafarina, *Phys. Rev. D* **88**, 064022 (2013) [arXiv:1307.2106 [gr-qc]].
- [28] P. S. Joshi, D. Malafarina and R. Narayan, *Class. Quant. Grav.* **31**, 015002 (2014) [arXiv:1304.7331 [gr-qc]].
- [29] R. Narayan and J. E. McClintock, *New Astron. Rev.* **51**, 733 (2008) [arXiv:0803.0322 [astro-ph]].
- [30] A. E. Broderick, A. Loeb and R. Narayan, *Astrophys. J.* **701**, 1357 (2009) [arXiv:0903.1105 [astro-ph.HE]].
- [31] M. A. Abramowicz, W. Kluzniak and J. -P. Lasota, *Astron. Astrophys.* **396**, L31 (2002) [astro-ph/0207270].
- [32] C. Bambi, *The Scientific World Journal* **2013**, 204315 (2013) [arXiv:1205.4640 [gr-qc]].
- [33] S. Doeleman, J. Weintroub, A. E. E. Rogers, R. Plambeck, R. Freund, R. P. J. Tilanus, P. Friberg and L. M. Ziurys *et al.*, *Nature* **455**, 78 (2008) [arXiv:0809.2442 [astro-ph]].
- [34] S. Doeleman, E. Agol, D. Backer, F. Baganoff, G. C. Bower, A. Broderick, A. Fabian and V. Fish *et al.*, arXiv:0906.3899 [astro-ph.CO].
- [35] S. Chandrasekhar, *The Mathematical Theory of Black Holes* (Clarendon Press, Oxford, UK, 1983).
- [36] H. Falcke, F. Melia and E. Agol, *Astrophys. J.* **528**, L13 (2000) [astro-ph/9912263].
- [37] C. Bambi and K. Freese, *Phys. Rev. D* **79**, 043002 (2009) [arXiv:0812.1328 [astro-ph]].
- [38] C. Bambi, K. Freese and R. Takahashi, in *Windows on the Universe*, edited by L. Celnikier et al. (The Gioi Publishers, Ha Noi, Vietnam, 2010), pp. 575-578 [arXiv:0908.3238 [astro-ph.HE]].
- [39] C. Bambi and N. Yoshida, *Class. Quant. Grav.* **27**, 205006 (2010) [arXiv:1004.3149 [gr-qc]].
- [40] L. Amarilla, E. F. Eiroa and G. Giribet, *Phys. Rev. D* **81**, 124045 (2010) [arXiv:1005.0607 [gr-qc]].
- [41] T. Johannsen and D. Psaltis, *Astrophys. J.* **718**, 446 (2010) [arXiv:1005.1931 [astro-ph.HE]].
- [42] C. Bambi, F. Caravelli and L. Modesto, *Phys. Lett. B* **711**, 10 (2012) [arXiv:1110.2768 [gr-qc]].
- [43] L. Amarilla and E. F. Eiroa, *Phys. Rev. D* **85**, 064019 (2012) [arXiv:1112.6349 [gr-qc]].
- [44] L. Amarilla and E. F. Eiroa, *Phys. Rev. D* **87**, 044057 (2013) [arXiv:1301.0532 [gr-qc]].
- [45] C. Bambi, *Phys. Rev. D* **87**, 107501 (2013) [arXiv:1304.5691 [gr-qc]].
- [46] S. -W. Wei and Y. -X. Liu, *JCAP* **1311**, 063 (2013) [arXiv:1311.4251 [gr-qc]].
- [47] H. Falcke and S. B. Markoff, *Class. Quant. Grav.* **30**, 244003 (2013) [arXiv:1311.1841 [astro-ph.HE]].
- [48] Z. Li and C. Bambi, *JCAP* **1401**, 041 (2014) [arXiv:1309.1606 [gr-qc]].
- [49] K. Hioki and K. -i. Maeda, *Phys. Rev. D* **80**, 024042 (2009) [arXiv:0904.3575 [astro-ph.HE]].
- [50] Z. Li, L. Kong and C. Bambi, arXiv:1401.1282 [gr-qc].
- [51] E. Ayon-Beato and A. Garcia, *Phys. Lett. B* **493**, 149 (2000) [gr-qc/0009077].

- [52] C. Bambi and L. Modesto, *Phys. Lett. B* **721**, 329 (2013) [arXiv:1302.6075 [gr-qc]].
- [53] A. E. Broderick, A. Loeb and M. J. Reid, *Astrophys. J.* **735**, 57 (2011) [arXiv:1104.3146 [astro-ph.HE]].
- [54] K. Liu, N. Wex, M. Kramer, J. M. Cordes and T. J. W. Lazio, *Astrophys. J.* **747**, 1 (2012) [arXiv:1112.2151 [astro-ph.HE]].